PNAS RESEARCH ARTICLE | ENVIRONMENTAL SCIENCES CELL BIOLOGY OPEN ACCESS

Mono-(2-ethyl-5-hydroxyhexyl) phthalate promotes uterine leiomyoma cell survival through tryptophan-kynurenine-AHR pathway activation

Takashi Iizuka[a], Ping Yin[a], Azna Zuberi[a], Stacy Kujawa[a], John S. Coon V[a], Richelle D. Björvang[b], Pauliina Damdimopoulou[b], Diana C. Pacyga[c], Rita S. Strakovsky[c], Jodi A. Flaws[d], and Serdar E. Bulun[a,1]

Edited by Thomas Spencer, University of Missouri, Columbia, MO; received June 14, 2022; accepted October 3, 2022

Uterine leiomyoma is the most common tumor in women and causes severe morbidity in 15 to 30% of reproductive-age women. Epidemiological studies consistently indicate a correlation between leiomyoma development and exposure to endocrine-disrupting chemical phthalates, especially di-(2-ethylhexyl) phthalate (DEHP); however, the underlying mechanisms are unknown. Here, among the most commonly encountered phthalate metabolites, we found the strongest association between the urine levels of mono(2-ethyl-5-hydroxyhexyl) phthalate (MEHHP), the principal DEHP metabolite, and the risk of uterine leiomyoma diagnosis ($n = 712$ patients). The treatment of primary leiomyoma and smooth muscle cells ($n = 29$) with various mixtures of phthalate metabolites, at concentrations equivalent to those detected in urine samples, significantly increased cell viability and decreased apoptosis. MEHHP had the strongest effects on both cell viability and apoptosis. MEHHP increased cellular tryptophan and kynurenine levels strikingly and induced the expression of the tryptophan transporters SLC7A5 and SLC7A8, as well as, tryptophan 2,3-dioxygenase (TDO2), the key enzyme catalyzing the conversion of tryptophan to kynurenine that is the endogenous ligand of aryl hydrocarbon receptor (AHR). MEHHP stimulated nuclear localization of AHR and up-regulated the expression of CYP1A1 and CYP1B1, two prototype targets of AHR. siRNA knockdown or pharmacological inhibition of SLC7A5/SLC7A8, TDO2, or AHR abolished MEHHP-mediated effects on leiomyoma cell survival. These findings indicate that MEHHP promotes leiomyoma cell survival by activating the tryptophan-kynurenine-AHR pathway. This study pinpoints MEHHP exposure as a high-risk factor for leiomyoma growth, uncovers a mechanism by which exposure to environmental phthalate impacts leiomyoma pathogenesis, and may lead to the development of novel druggable targets.

leiomyoma | endocrine-disrupting chemicals | phthalate | tryptophan | aryl hydrocarbon receptor

Uterine leiomyoma (LM) is the most common gynecological benign smooth muscle tumor originating from the uterine myometrium (MM) (1). Almost 80% of reproductive-age women will develop at least one LM by 50 y of age (2). Approximately 200,000 hysterectomies and 30,000 myomectomies are performed annually in the United States to alleviate the serious health complications associated with LM, with an estimated cost of $5.9 to $34.4 billion (3). LM is a hormone-dependent tumor, with both estrogen and progesterone involved in tumor growth (4). Risk factors for LM include age, race, reproductive factors (parity, menarche), hormone levels, obesity, lifestyle, diet, and genetic factors (5).

Endocrine-disrupting chemicals (EDCs) are defined as exogenous chemicals or a mixture of chemicals that interfere with the endocrine system and alter hormone activity. EDCs were once thought to function by manipulating nuclear hormone receptors, such as estrogen receptors, androgen receptors, progesterone receptors, thyroid receptors, and retinoid receptors (6); however, research has since revealed that the mechanisms of EDC effects are much broader than initially recognized. EDCs have been shown to affect the functions of nonsteroid receptors (e.g., neurotransmitter receptors) and other nuclear receptors (e.g., aryl hydrocarbon receptor [AHR]), and interfere with enzymatic pathways involved in steroid biosynthesis and metabolism in the endocrine and reproductive systems (6, 7). Phthalates are known EDCs; they are commonly referred to as plasticizers and are used to increase the durability of plastics. Phthalates are found in hundreds of products, including personal care products (soaps, shampoos, and hair sprays), food packaging, and medical products (8). Di-(2-ethylhexyl) phthalate (DEHP) is a common plasticizer found in medical products. The general public can be exposed to DEHP through ingestion of food, drink, or dust that has come in contact with materials containing DEHP, or through inhalation of contaminated air (9). Individuals treated with medical products containing DEHP are at risk for exposure to high levels of DEHP (10). Urinary phthalate metabolite concentrations are the

Significance

Uterine leiomyomas (or fibroids) represent the most common tumor affecting up to 80% of reproductive-age women. Epidemiological studies consistently indicate a positive association between exposure to endocrine-disrupting phthalates and leiomyoma risk; however, the underlying mechanisms remain unclear. Here, we demonstrate that the ubiquitous environmental pollutant mono-(2-ethyl-5-hydroxyhexyl) phthalate [MEHHP, the major metabolite of di-(2-ethylhexyl) phthalate] promotes leiomyoma cell survival through increasing cellular tryptophan uptake, kynurenine production, and aryl hydrocarbon receptor pathway activation. Both epidemiologically and mechanistically, our study identified MEHHP exposure as a high-risk factor for leiomyoma growth. These findings are expected to open new avenues in the leiomyoma research field and facilitate the development of novel intervention strategies for the treatment or prevention of the disease.

Author contributions: T.I., P.Y., J.A.F., and S.E.B. designed research; T.I., A.Z., S.K., and J.S.C. performed research; T.I., P.Y., R.D.B., P.D., D.C.P., R.S.S., J.A.F., and S.E.B. analyzed data; and T.I., P.Y., and S.E.B. wrote the paper.

The authors declare no competing interest.

This article is a PNAS Direct Submission.

[1]To whom correspondence may be addressed. Email: s-bulun@northwestern.edu.

This article contains supporting information online at http://www.pnas.org/lookup/suppl/doi:10.1073/pnas.2208886119/-/DCSupplemental.

Published November 14, 2022.

preferred biomarkers of phthalate exposure. Humans are exposed to phthalate diesters (i.e., parent compounds), which are rapidly metabolized to monoester metabolites in the body. Therefore, epidemiological studies measuring human urinary phthalate metabolites often measure one or more metabolites for each parent phthalate and report sums of metabolite concentrations based on parent compound, exposure source, or biological activity (11). DEHP is metabolized by various tissues to more bioactive metabolites, including mono(2-ethyl-5-hexyl) phthalate (MEHP), mono(2-ethyl-5-oxohexyl) phthalate (MEOHP), mono(2-ethyl-5-hydroxyhexyl) phthalate (MEHHP), and mono(2-ethyl-5-carboxypentyl) phthalate (MECPP) (12). Urinary concentrations of these metabolites are measured to evaluate the exposure to DEHP. Studies have shown that DEHP and its metabolites influence steroid hormone levels and reproductive organ development and function (13, 14).

Recently, an association between phthalate exposure and LM growth has been established. Epidemiological studies have shown that higher urinary concentrations of phthalates, especially DEHP and its metabolites, correlate with an increase in total LM burden (uterine volume and LM size) (15), increased risk of LM (16, 17), and increased microRNA expression associated with cellular processes favoring LM growth (18). Experimental studies have shown that DEHP increases LM cell viability and decreases apoptosis (19, 20). It was proposed that EDCs may affect LM growth by interfering with the action of estrogen and progesterone, two steroid hormones critical for LM growth (21); however, the detailed cellular and molecular mechanisms underlying EDC-associated LM growth are not well understood.

AHR is a nuclear receptor that acts as a ligand-activated transcription factor (22). The metabolites of tryptophan, including kynurenine, kynurenic acid, and tryptamine, have been reported to be endogenous AHR ligands (23, 24). Several EDCs act as exogenous AHR agonists, including 2,3,7,8-tetrachlorodibenzo-p-dioxin (TCDD), polychlorinated biphenyls (PCBs), and polycyclic aromatic hydrocarbons (25). Among these ligands, kynurenine and TCDD are the strongest activators of AHR (26, 27). Ligand-bound AHR forms a heterodimer with the AHR nuclear transactivator (ARNT) and binds to xenobiotic response elements at the target gene regulatory sites, inducing their expression. Studies have shown that phthalates can affect tryptophan metabolism (28, 29) and activation of the AHR pathway (30, 31), both of which play important roles in regulating cell proliferation, cell cycle, apoptosis, differentiation, metabolism, and tumorigenesis (32). Recently, we and others reported the involvement of dysregulated tryptophan metabolism in the pathogenesis of LM; however, the mechanisms involved remain to be elucidated (33, 34). In this study, we investigated the effects of phthalates on LM cell function, testing the hypothesis that MEHHP (the major metabolite of DEHP) supports LM cell survival through the promotion of tryptophan metabolism and activation of the AHR pathway.

Results

Determination of the Phthalate Metabolites for In Vitro Studies Based on In Vivo Association of Urinary Phthalate Metabolites with Uterine LM Risk. The formulas and composition of phthalate metabolite mixtures used in this study are summarized in *SI Appendix*, Fig. S1 and Table S1. We determined the composition of these mixtures based on urinary metabolite concentrations of phthalates reported in the Midlife Women's Health Study (MWHS), which assessed the association between urinary phthalate metabolite concentrations and women's health conditions in a prospective cohort of pre- and perimenopausal women from Baltimore and its surrounding counties (35, 36). The concentrations of individual urinary phthalate metabolites and DEHP molar sums of the MWHS study are summarized in *SI Appendix*, Table S2. For this study, the exposure-based epidemiological (EPI) mixture included nine phthalate metabolites at concentrations equivalent to their urinary concentrations (*SI Appendix*, Table S1). The effect-based "bad actor" (BAD) mixture comprised the top four phthalate metabolites associated with serum estradiol concentration based on the Weighted Quantile Sum (WQS) model ($P = 0.05$) (*SI Appendix*, Fig. S2*A*). The weights for each component of the BAD mixture were: MEHHP: 22%; MiBP (monoisobutyl phthalate): 21%; MEP (monoethyl phthalate): 21%; and MBzP (monobenzyl phthalate): 16% (*SI Appendix*, Fig. S2*B*). Both the EPI and BAD mixtures contained MEHHP.

We also wanted to examine the effects of single phthalate metabolites on LM cell function. To narrow down the candidate metabolites to be evaluated in vitro, we analyzed the MWHS data and assessed associations of urinary concentrations of nine phthalate metabolites (MEHP, MEHHP, MEOHP, MECPP, MCPP, MBzP, MEP, MBP, and MiBP) as a mixture with risk of LM diagnosis to identify which metabolites were potentially the most notable contributors (35, 36). We demonstrated that women with LMs had significantly higher mean concentrations of MEHHP, MEOHP, MEP, and MiBP than those without LMs (*SI Appendix*, Table S3). Overall, the phthalate metabolite mixture was positively associated with prior LMs diagnosis, such that 10% increases in urinary concentrations of all nine metabolites were associated with 6.0% higher risk of prior LMs diagnosis (risk ratio [RR] = 1.06; 95% confidence interval [CI] = 1.00, 1.12; $P = 0.04$). The largest contributors to this association were MEHHP (26.6%), MiBP (17.7%), MEP (12.3%), and MEOHP (12.1%) (Fig. 1). These findings indicated the DEHP metabolite MEHHP as a particularly high-risk factor for LM growth. Previous studies have reported the positive association of DEHP exposure with LM risk (16, 17). Thus, we evaulated MEHHP and DEHP as single compounds in the following mechanistic studies.

The low-dose (*SI Appendix*, Table S1) and medium-dose (10× low dose) of mixtures and single compounds used in our study fell within the range of, or close to, the levels in clinical urinary samples reported in the MWHS study, making our study relevant to environmental health (36). All compounds were dissolved in dimethyl sulfoxide (DMSO), which was used as the vehicle control.

Phthalates Increase Viability and Decrease Apoptosis in LM cells. We evaluated the biological effects of phthalates on primary LM smooth muscle cell viability, apoptosis, and direct cytotoxicity using the ApoTox-Glo Triplex Assay. Overall, treatment with MEHHP showed the strongest biological effects; the effects of MEHHP are thus highlighted in the main text figures, whereas the effects of EPI/BAD mixtures or DEHP are shown in *SI Appendix*. Treatment of LM cells with MEHHP at various doses for 48 h and 72 h significantly increased cell viability (represented by the total number of living cells) compared with vehicle-treated cells (Fig. 2*A*). Treatment with EPI or BAD mixtures or DEHP showed increased cell viability, but these differences did not reach statistical significance (*SI Appendix*, Fig. S3*A*). Apoptosis of LM cells was decreased by treatment with individual phthalates or defined phthalate mixtures (*SI Appendix*, Fig. S3*B*); the medium-dose concentration of MEHHP showed the significant effect (Fig. 2*B*). Annexin V staining followed by flow cytometry analysis confirmed that medium-dose MEHHP significantly decreased the population of apoptotic cells (Fig. 2 *D* and *E*). These treatments

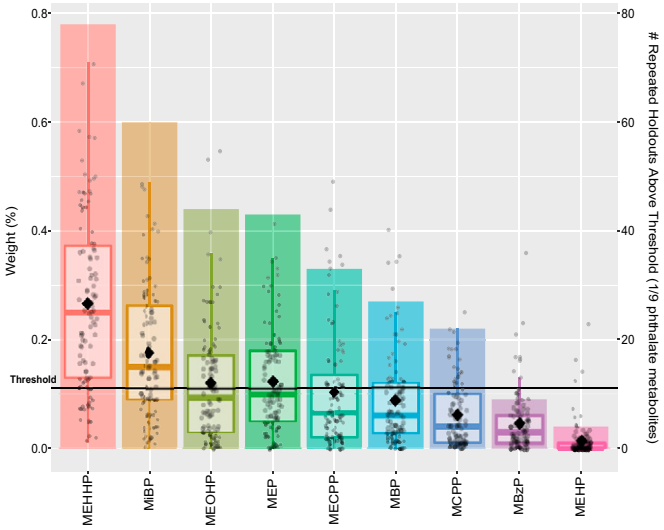

Fig. 1. Relative importance of urinary phthalate metabolites to the overall association of the metabolite mixture with prior LM diagnosis. WQSR models, which were constrained in the positive direction, evaluated associations between the mixture and the risk of having (n = 193) compared to not having (n = 519) a prior LM diagnosis (RR = 1.06; 95% CI = 1.00, 1.12; P = 0.04). Boxplots present the distributions of relative weights for each metabolite from 100 repeated holdouts where each dot is a weight from one repeated holdout, the diamonds indicate the mean, and bar height indicates the proportion of repeated holdouts with weights above the threshold (1 of 9 phthalate metabolites or 11.1%). Notable metabolite contributors to the overall mixture association are those with diamonds above the threshold.

did not induce any direct cytotoxicity in LM cells, except for the medium and high doses of DEHP (Fig. 2*C* and *SI Appendix*, Fig. S3*C*). We also treated MM cells with MEHHP. MEHHP did not increase the cell viability (*SI Appendix*, Fig. S4*A*). MEHHP decreased apoptosis (*SI Appendix*, Fig. S4*B*), but the effect was weaker or variable compared with LM cells.

Next, we assessed whether various phthalate metabolites altered cell proliferation. The BrdU incorporation assay revealed that only MEHHP treatment slightly increased the percentage of S-phase cells, but this trend did not reach statistical significance (Fig. 2 *F* and *G*). There was no difference in other cell cycle parameters between the vehicle- and MEHHP-treated groups (*SI Appendix*, Fig. S3*D*). In previous reports, DEHP promoted the production of extracellular matrix (ECM) and fibrosis of the liver (37). Because ECM production is one of the hallmarks of LM growth, we assessed the ECM gene expression by MEHHP. We demonstrated that COL1A1 and COL3A1 mRNA levels were significantly up-regulated by MEHHP treatment (*SI Appendix*, Fig. S5).

Taken together, these data suggest that the DEHP metabolite MEHHP increases cell viability primarily via reducing apoptosis and thus represents a high-risk factor for LM growth.

MEHHP Promotes LM Cell Survival through Activation of the AHR Pathway. The function of AHR as an environmental sensor that responds to environmental pollutants prompted us to examine whether MEHHP affects AHR activation in LM cells. MEHHP treatment led to robust nuclear translocation of AHR in primary LM cells (Fig. 3 *A* and *B*). Quantification of the AHR^+ nuclear area confirmed that MEHHP significantly increased the nuclear accumulation of AHR, comparable to that induced by the strong AHR agonist TCDD (Fig. 3*C*). MEHHP treatment also significantly up-regulated mRNA levels of CYP1A1 and CYP1B1, two AHR target genes and classic markers of AHR activation (38, 39), suggesting that MEHHP triggers the AHR pathway (Fig. 3*D*). Additionally, MEHHP moderately increased AHR gene expression. We also evaluated the CYP1B1 transcriptional level in LM and MM tissue to assess AHR activation in these tissues. CYP1B1 mRNA levels were higher in LM tissue than MM tissue (*SI Appendix*, Fig. S6*A*), indicating the activation of the AHR pathway in LM tissue.

We performed AHR knockdown to investigate whether MEHHP supports cell survival through the AHR pathway. We used two different small-interfering RNAs (siRNAs; si-AHR_1 and si-AHR_2), and both significantly down-regulated AHR mRNA (Fig. 3*E*) and protein levels (*SI Appendix*, Fig. S6 *B* and *C*). Knockdown of AHR also decreased the mRNA levels of its target genes CYP1A1 and CYP1B1, indicating that AHR knockdown had functional consequences. MEHHP treatment increased cell viability in control siRNA-transfected cells, but these effects were significantly reduced in cells with AHR knockdown (Fig. 3*F*). AHR knockdown also reversed the MEHHP-induced reduction in apoptosis, with increased apoptosis in the cells with higher AHR knockdown efficiency (Fig. 3*G*). Furthermore, blocking AHR action with the AHR-specific antagonist CH223191 significantly reduced the antiapoptotic effect of MEHHP (Fig. 3*H*). These findings suggest that MEHHP supports LM cell survival through activation of the AHR pathway.

MEHHP Activates the AHR Pathway through Promotion of Cellular Tryptophan Uptake and Kynurenine Production. It was previously suggested that DEHP might interfere with tryptophan metabolism (29). Here, we used an unbiased approach to investigate the effects of MEHHP on the levels of cellular tryptophan and its downstream metabolites using liquid chromatography-mass spectrometry (LC-MS) (Fig. 4*A*). Among all the compounds measured, MEHHP significantly and strikingly increased the cellular levels of only tryptophan and kynurenine compared with vehicle-treated LM cells (Fig. 4 *B* and *C*). MEHHP treatment was associated with higher levels of quinolinic acid (QA) in all five LM cell samples, whereas 3-hydroxykynurenine (3-HK) and xanthurenic acid (XA) levels were higher in four of five LM samples treated with MEHHP. Alterations in QA, 3-HK, or XA levels did not reach statistical significance, however.

Based on this metabolomic analysis, we assessed whether MEHHP enhances tryptophan uptake in primary LM cells. In mammalian cells, transporter-mediated tryptophan uptake occurs mainly via the neutral amino acid transporter System L, a heterodimer composed of a heavy glycoprotein chain (CD98, encoded by *SLC3A2*) and one of two catalytic L chains, LAT1 or LAT2, encoded by *SLC7A5* or *SLC7A8*, respectively (Fig. 4*A*) (40, 41). We and others have previously reported that these transporter genes are up-regulated in LM compared with MM tissue (42, 43). The published RNA-sequencing data (44–46) involving fibroid tissues and matched adjacent myometrial samples supported these earlier reports and showed that SLC7A5 mRNA levels are significantly higher in LM tissue, whereas SLC7A8 mRNA levels showed a similar trend (*SI Appendix*, Fig. S7*A*). We found that MEHHP treatment of LM cells significantly increased SLC7A5 and SLC7A8 mRNA levels after 8 h, and increased tryptophan 2,3-dioxygenase (TDO2) mRNA after 24 h (Fig. 4*D*). We demonstrated that MEHHP treatment increased SLC7A5 protein levels (Fig. 4 *E* and *F*). These findings suggest that MEHHP promotes tryptophan metabolism toward kynurenine production through an increase in cellular tryptophan uptake and metabolism.

Next, we performed knockdown of SLC7A5 and SLC7A8 to determine whether they affect MEHHP-mediated LM cell survival. To address their redundant functions (47), we transfected LM cells with specific siRNAs targeting SLC7A5 and SLC7A8

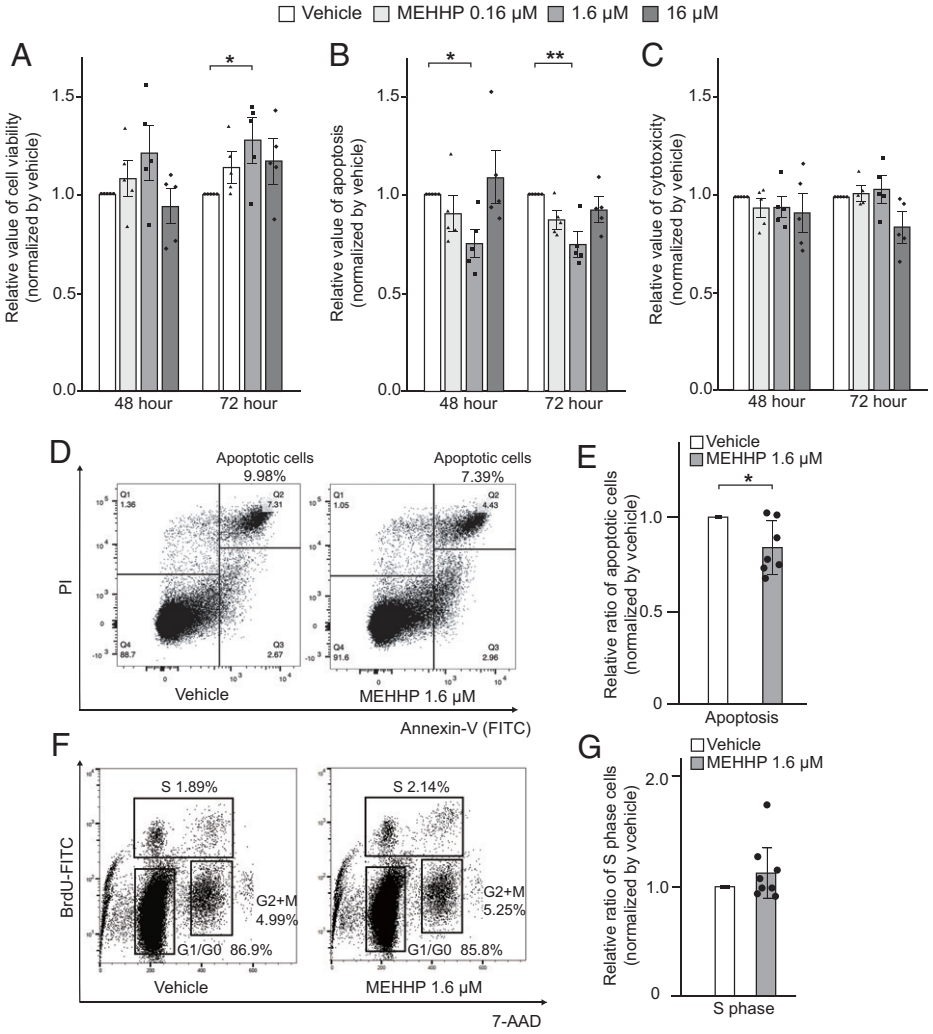

Fig. 2. MEHHP increases viability and decreases apoptosis in LM cells. (*A*–*C*) LM cells were treated with vehicle or various concentrations of MEHHP (0.16, 1.6, 16 μM) for 48 or 72 h. Cell viability (*A*), apoptosis (*B*), and cytotoxicity (*C*) were assessed using the ApoTox-Glo Triplex Assay kit. Values are presented as mean ± SEM ($n = 5$). (*D*) Representative flow cytometry plots showing the percentage of apoptotic cells. LM cells were treated with vehicle or MEHHP (1.6 μM) for 48 h followed by Annexin-V and PI staining and flow cytometry analysis. (*E*) Bar graph showing the relative ratio of apoptotic LM cells after treatment with MEHHP vs. vehicle. Values are presented as mean ± SEM ($n = 7$). (*F*) Representative flow cytometry plots showing the distribution of LM cells in different phases of the cell cycle. Cells were treated with vehicle or MEHHP (1.6 μM) for 72 h and BrdU was added for the last 24 h. The cells were analyzed by flow cytometry. (*G*) Bar graph showing the relative ratio of LM cells in S phase after treatment with MEHHP vs. vehicle. Values are presented as mean ± SEM ($n = 8$). Statistical analysis was performed using Student's *t* test or Dennett's multiple comparison test compared with vehicle control. $^{*}P < 0.05$, $^{**}P < 0.01$.

simultaneously, which significantly down-regulated the mRNA levels of both genes (Fig. 5*A*) and SLC7A5 protein levels (*SI Appendix*, Fig. S7 *B* and *C*). Incubation with tryptophan increased LM cell viability and decreased apoptosis, but knockdown of SLC7A5/7A8 significantly reduced the effects of tryptophan on cell viability (Fig. 5*B*) and apoptosis (Fig. 5*C*), verifying that transporter-induced tryptophan uptake supports LM cell survival. Similarly, the effects of MEHHP on LM cell survival were also abolished by knockdown of SLC7A5 and SLC7A8 (Fig. 5 *D* and *E*). Furthermore, we investigated the role of TDO2 in MEHHP-induced LM cell survival by knocking down TDO2 using two different siRNAs (Fig. 5*F*). TDO2 knockdown moderately but significantly reduced the effects of MEHHP on cell viability and apoptosis (Fig. 5 *G* and *H*). Treatment with the TDO2 inhibitor 680C91 also reduced the antiapoptotic effect of MEHHP on LM cells (*SI Appendix*, Fig. S7*D*). Taken together, these findings suggest that MEHHP supports LM cell survival by promoting the cellular uptake of tryptophan, which is then converted by TDO2 to kynurenine for the activation of AHR.

Discussion

We demonstrated that exposure to mixtures of phthalate metabolites or the single compound MEHHP (the major DEHP metabolite) can increase LM cell survival and risk of development of LMs or induction of their growth. MEHHP treatment of LM cells up-regulated the expression of amino acid transporters SLC7A5 and SLC7A8, as well as the critical tryptophan catabolic enzyme TDO2, which together stimulate cellular tryptophan uptake and kynurenine production, leading to increased AHR activation and LM cell survival (Fig. 6). Our data identified MEHHP exposure as a critical risk factor for LM growth via activation of the tryptophan-kynurenine-AHR pathway.

The effects of phthalate metabolites on LM cells did not show a linear dose–response. The effects were the strongest at medium-range doses, showing a U-shaped dose–response curve (Fig. 2 *A* and *B*). These nonmonotonic dose–response curves (NMDRCs) are commonly seen in studies of the effects of EDCs, such as phthalates. Several mechanisms may contribute

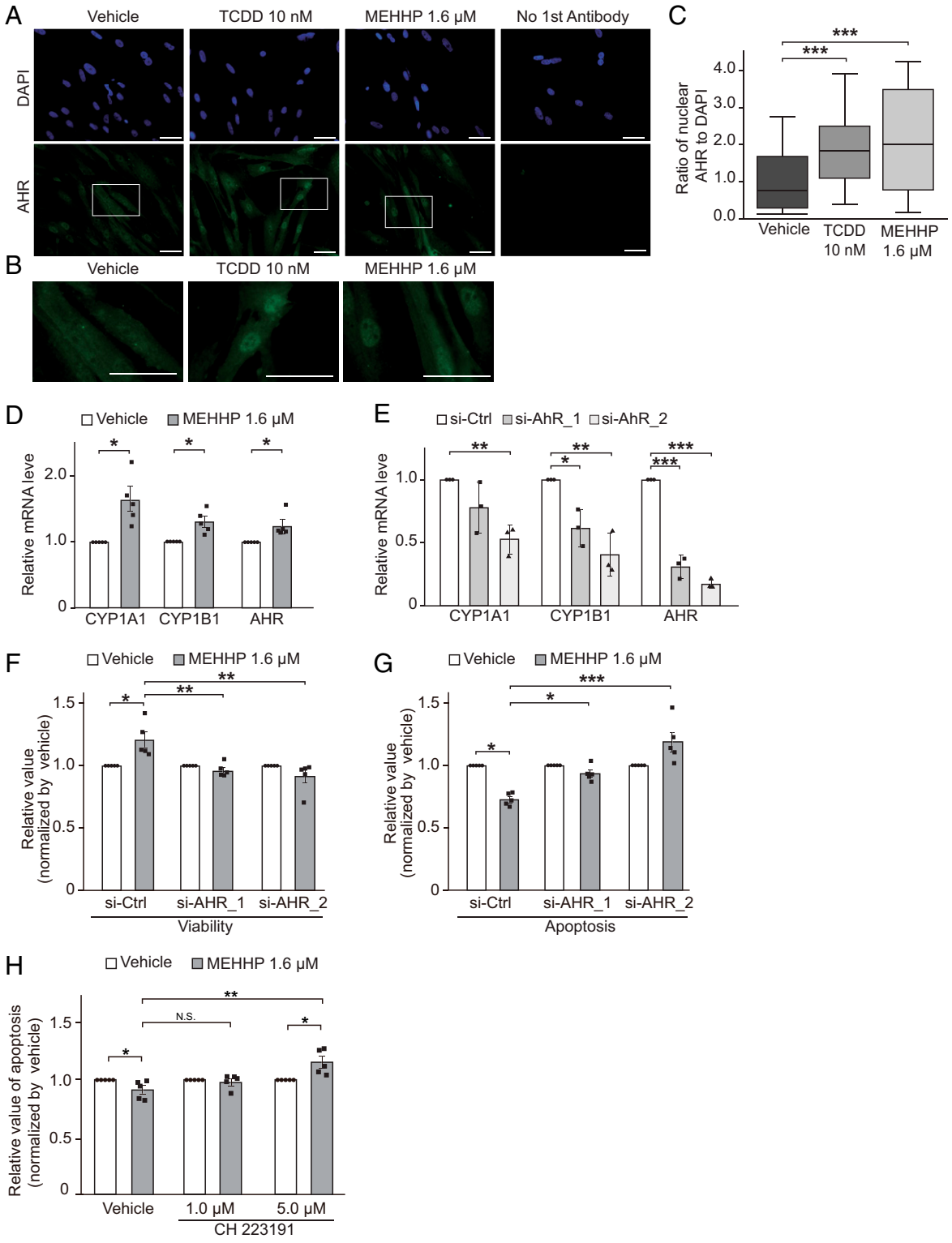

Fig. 3. MEHHP promotes LM cell survival through activation of the AHR pathway. (*A*) Representative images of immunocytochemistry staining for AHR (green) in LM cells treated with vehicle (DMSO), TCDD (10 nM), or MEHHP (1.6 μM) for 24 h. DAPI was used for nuclear staining (blue). (Scale bars, 100 μm.) (*B*) High-magnification images of cells highlighted in *A*. (Scale bars, 100 μm.) (*C*) The relative ratio of the AHR-positive nuclear area normalized to the DAPI-stained nuclear area quantified by ImageJ. Statistical analysis was performed using the Kruskal–Wallis test compared with vehicle control ($n = 3$). ***$P <$ 0.001. (*D*) Bar graph showing RT-qPCR quantification of CYP1A1, CYP1B1, and AHR gene expression levels in LM cells treated with MEHHP (1.6 μM) or vehicle for 8 h. Values are presented as mean ± SEM ($n = 5$). (*E*) Bar graph showing RT-qPCR quantification of AHR, CYP1A1, and CYP1B1 gene expression levels in LM cells transfected with control siRNA (si-Ctrl) or two different AHR siRNAs (si-AHR_1 and si-AHR_2). Values are presented as mean ± SEM ($n = 3$). (*F* and *G*) The effects of AHR knockdown on MEHHP-induced cell survival in LM cells. The cells were transfected with control or AHR siRNAs for 24 h, followed by treatment with vehicle or MEHHP (1.6 μM) for 72 h. Cell viability (*F*) and apoptosis (*G*) were assessed by ApoTox-Glo Triplex Assay. Values were normalized to vehicle control and presented as mean ± SEM ($n = 5$). H: LM cells were treated with MEHHP in the presence or absence of the AHR-specific antagonist CH 223191 at 1 μM and 5 μM for 72 h. Apoptosis was assessed by evaluation of Caspase 3/7 activity. Values were normalized to vehicle control for each group and presented as mean ± SEM ($n = 5$). Statistical analysis was performed using Student's *t* test or Dennett's multiple comparison test compared with control. *$P < 0.05$, **$P < 0.01$, ***$P < 0.001$.

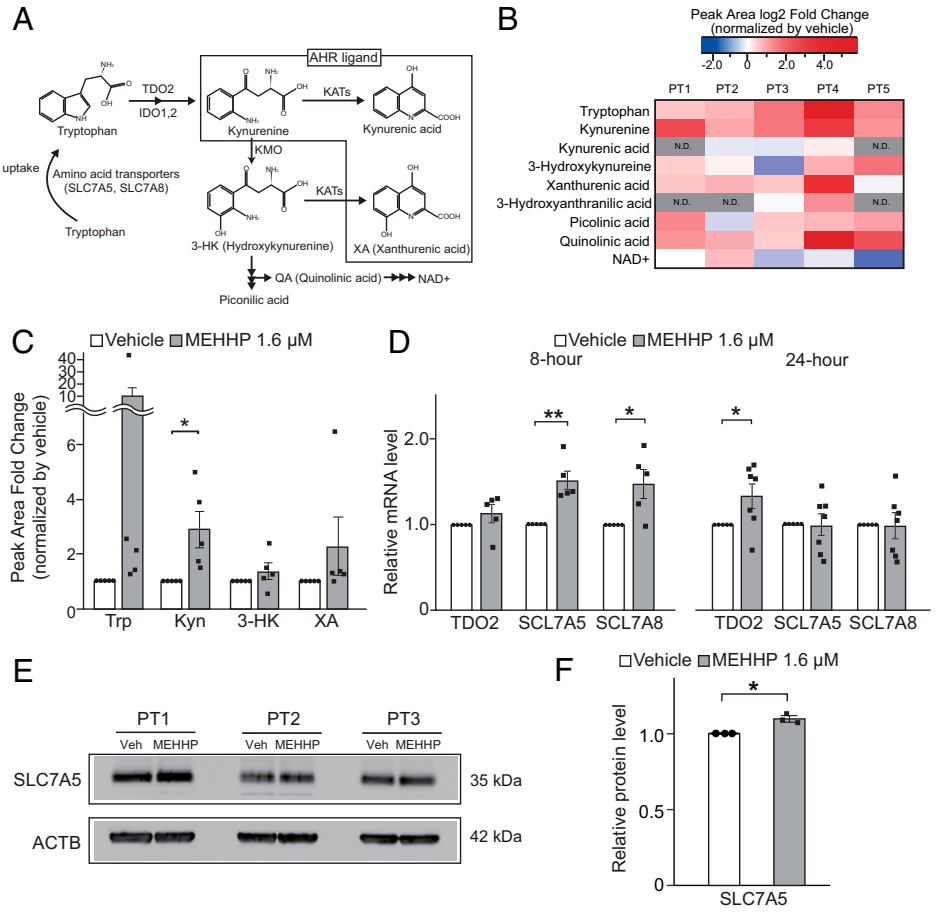

Fig. 4. MEHHP promotes tryptophan uptake and metabolism in LM cells. (*A*) Schematic diagram of the tryptophan-kynurenine metabolism pathway. IDO, indoleamine 2,3-dioxygenase; KATs, kynurenine aminotransferases; KMO, kynurenine 3-monooxygenase; NAD, nicotinamide adenine dinucleotide; SCL7A5, Solute Carrier Family 7 Member 5; SCL7A8, Solute Carrier Family 7 Member 8. (*B* and *C*) The levels of tryptophan and its metabolites in LM cells treated with MEHHP (1.6 μM) or vehicle for 72 h were assessed by LC-MS. The fold-change of peak area of each metabolite in MEHHP- vs. vehicle-treated cells is shown as a heat map (*B*) and histogram (*C*). Values are presented as mean ± SEM ($n = 5$). Trp, tryptophan; Kyn, kynurenine. (*D*) Gene expression in LM cells treated with MEHHP (1.6 μM) for 8 h ($n = 5$) or 24 h ($n = 8$). Values are presented as mean ± SEM. (*E*) Immunoblot image showing SLC7A5 protein expression in LM cells treated with MEHHP (1.6 μM). (*F*) ImageJ quantification of SLC7A5 protein levels in *E*. Values are presented as mean ± SD ($n = 3$). Statistical analysis was performed using paired *t* test compared with control. $^*P < 0.05$, $^{**}P < 0.01$.

to NMDRCs, including the cytotoxicity of the compounds, down-regulation and desensitization of receptors, and competition with endogenous ligands (48). Phthalate metabolites did not produce significant cytotoxicity in LM cells, suggesting that other factors account for the NMDRCs observed in these cells. The U-shaped dose–response curves observed indicate the complex effects of phthalate mixtures on LM cells.

Epidemiological studies consistently demonstrate correlations between urine levels of DEHP metabolites (especially MEHHP) and LM, despite differences in study populations and assessment methods (15–17). We found that MEHHP, but not its parent compound DEHP, supported LM cell survival in vitro. The effect of DEHP is thought to be attributed to its metabolites, such as MEHP and MEHHP, rather than DEHP itself (49). DEHP is hydrolyzed to MEHP and 2-ethylhexyanol (2-EH) by lipase, mainly in the liver, small intestine, and kidney (50, 51). MEHP is further metabolized to CYP-mediated oxidative and dealkylated metabolites, including MEHHP in the liver and intestine (51). Therefore, the effect of DEHP depends on the activity of these enzymes, which may be deficient in our primary LM cell culture system. Our results also showed that a single compound of MEHHP was the most potent compound to increase LM cell viability (Fig. 2*A*) and decrease apoptosis (Fig. 2*B*), even though the EPI and BAD mixture contained the same concentration of MEHHP (*SI Appendix*, Fig. S3 *A* and *B*). Because the phthalate metabolites are structurally similar, they can exhibit competitive effects on each other, resulting in overall decreased effectiveness in the mixture. It is also possible that the phthalate composition that is excreted in the urine may not represent the phthalate mixture within the uterus in vivo. The metabolizing enzymes of the local tissue determine which metabolite is predominant (51). This is why we conducted extensive dose–response and time-course studies using MEHHP, which was the most potent compound to increase LM cell viability (Fig. 2*A*). Without such information it is not possible to implicate the toxicity of a chemical or fully understand its mechanism of action.

We demonstrated that MEHHP promotes the nuclear translocation of AHR and stimulates the expression of AHR target genes CYP1A1 and CYP1B1. Knockdown of AHR by siRNA abolished MEHHP-induced LM cell survival, suggesting that MEHHP supports cell survival through activation of the AHR pathway in LM cells. Our findings are consistent with those of previous studies that reported an association between phthalate exposure and AHR pathway activation. Mankidy et al. (52) demonstrated that DEHP and other phthalates weakly activate AHR in a luciferase reporter assay. Shan et al. (31) found that MEHP stimulates AHR nuclear translocation and recruitment to its target gene promoter, induces AHR target gene expression, and promotes cell migration and invasion in MCF7 breast cancer cells. Despite these functional studies, the mechanisms underpinning phthalate-mediated AHR

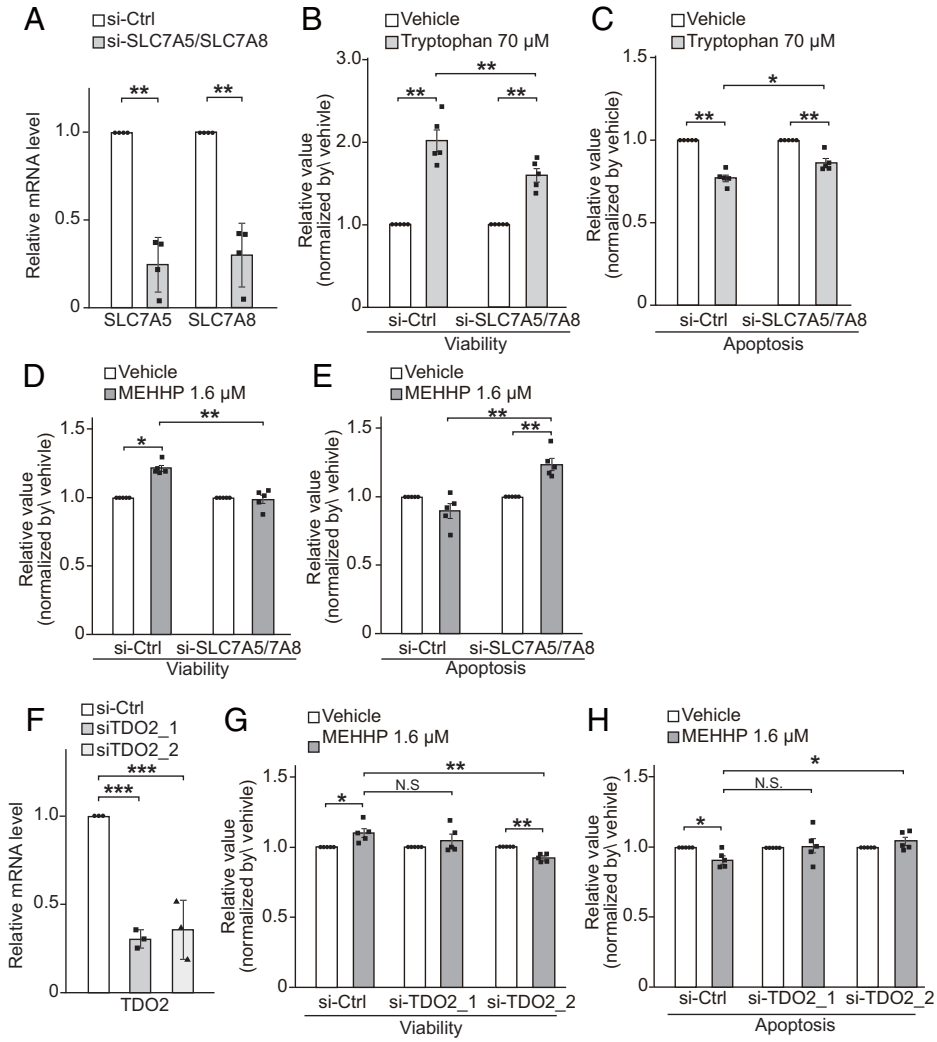

Fig. 5. Effects of blocking the tryptophan-kynurenine metabolism pathway on MEHHP-mediated LM cell survival. (*A*) Knockdown of SLC7A5 and SLC7A8 in LM cells significantly decreased their gene-expression levels as assessed by RT-qPCR ($n = 4$). (*B* and *C*) The effects of SLC7A5 and SLC7A8 knockdown on tryptophan-mediated LM cell survival. Twenty-four hours after siRNA transfection, LM cells were treated with vehicle (water) or 70 μM tryptophan for 72 h followed by assessment of cell viability (*B*) and apoptosis (*C*) by ApoTox-Glo Triplex Assay. Values were normalized to vehicle control for each group ($n = 5$). (*D* and *E*) The effects of SLC7A5 and SLC7A8 knockdown on MEHHP-mediated LM cell viability (*D*) and apoptosis (*E*). As in *B* and *C*, after siRNA transfection, LM cells were treated with vehicle or 1.6 μM MEHHP followed by analysis with the ApoTox-Glo Triplex Assay. Values were normalized to vehicle control for each group ($n = 5$). (*F*) Two different siRNAs for TDO2 (siTDO2_1, siTDO2_2) significantly decreased its gene expression in LM cells ($n = 3$). (*G* and *H*) Knockdown of TDO2 reduced the prosurvival effects of MEHHP on LM cells. The cells were transfected with siRNA and treated with MEHHP, followed by assessment with the ApoTox-Glo Triplex Assay for cell viability (*G*) and apoptosis (*H*) ($n = 5$). Values were normalized to vehicle control for each group. Values are presented as mean ± SEM. Statistical analysis was performed using Student's *t* test or Dennett's multiple comparison test compared with control. $*P < 0.05$, $**P < 0.01$, $***P < 0.001$.

activation remain unclear. Intriguingly, we found that MEHHP treatment increased tryptophan and kynurenine levels in LM cells. Kynurenine acts as an endogenous ligand of AHR, which plays important roles in antiapoptotic processes, by stimulating the expression of interleukin (IL)-1β, interleukin (IL)-8, cyclooxygenase (COX)-2, and NF-κB subunit RelB (53–55). Under the conditions of robust AHR suppression, MEHHP induced apoptosis (Fig. 3 *G* and *H*). We speculate that MEHHP-enhanced apoptosis in the presence of profound AHR suppression was due to perturbing the balance between AHR and an alternative pathway (56, 57).

Consistent with elevated cellular tryptophan and kynurenine levels, MEHHP treatment stimulated the expression of amino acid transporters SLC7A5 and SLC7A8 that are responsible for tryptophan uptake in mammalian cells and TDO2, which is the key and rate-limiting enzyme catalyzing the conversion of tryptophan to kynurenine. Depletion of SLC7A8 and SLC7A5 or blocking TDO2 function with inhibitors significantly reduced the effects of MEHHP on LM cell survival. Together, these findings strongly suggest that MEHHP activates the AHR pathway and supports LM cell survival at least partially via promoting cellular tryptophan uptake and kynurenine production. In addition, recent studies have revealed that LM tissue exhibited higher TDO2, SLC7A5, SLC7A8, and CYP1B1 gene expression, and higher kynurenine levels compared with MM tissue (33, 34, 58). The AHR pathway in fibroid tissue is activated and leads to higher CYP1B1 expression (*SI Appendix*, Fig. S6*A*), because of higher levels of tryptophan-uptake and its downstream product kynurenine. In contrast to its consistent effect on LM cells, MEHHP did not increase the MM cell viability (*SI Appendix*, Fig. S4*A*) and showed weaker or variable effects on apoptosis (*SI Appendix*, Fig. S4*B*). These differences with respect to the MEHHP effect between LM and MM cells may be due to strikingly lower activation of the tryptophan-kynurenine-AHR pathway in MM cells.

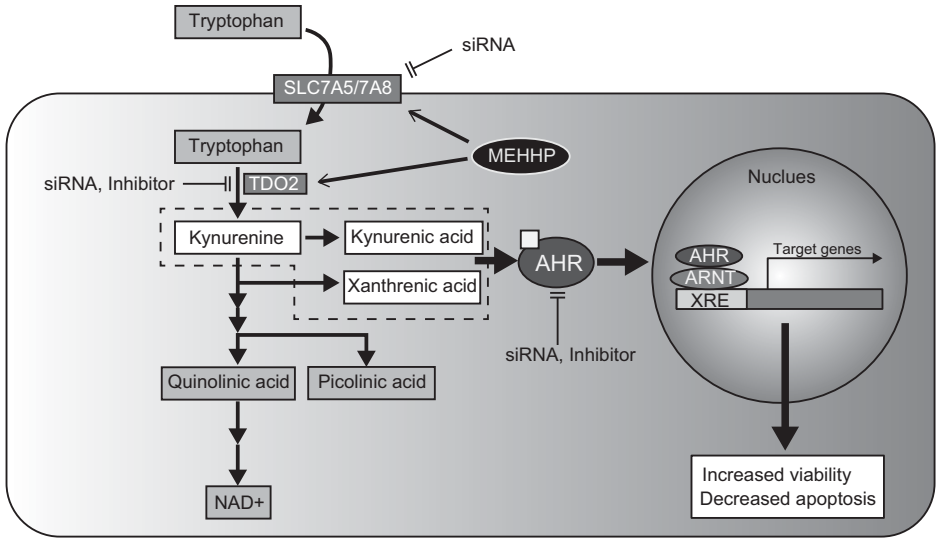

Fig. 6. Schematic of MEHHP effect in LM cells. MEHHP stimulates tryptophan metabolism and increases AHR ligand production, which activates the AHR pathway and contributes to LM cell survival. XRE, Xenobiotic response element.

Previous studies have shown that phthalates and their metabolites inhibit the activity of aminocarboxymuconate semialdehyde decarboxylase (ACMSD) (29) and quinolinate phosphoribosyl transferase (QPRT) (59), two enzymes downstream of TDO2 in the tryptophan-kynurenine metabolism pathway, leading to increased QA levels in exposed animals (29, 60). Whether this mechanism also contributes to the altered tryptophan metabolite levels in LM cells warrants further study.

Importantly, we used LM cells harvested from human tissue rather than cell lines to perform these experiments, thus increasing the physiological relevance of our findings. We observed consistent effects of MEHHP on cell viability and apoptosis in LM cells isolated from different patient samples, although the extent of the effects (not surprisingly) varied between LM samples from individual subjects. Exposure to EDCs, especially DEHP, has long been reported to be a risk factor for LM, and Black women, who are more likely to develop LM, also have higher levels of environmental exposure to EDCs (61–64). Nonetheless, the influence of these chemicals on LM pathogenesis is understudied (65).

We have provided mechanistic evidence that the DEHP metabolite MEHHP is a critical risk factor for LM growth via the activation of the tryptophan-kynurenine-AHR axis, a key pathway involved in tumorigenesis in various tissues. One limitation of our study is that we primarily focused on defining the in vitro effects of one candidate DEHP metabolite, MEHHP, on LM cells, which does not mimic the exposure to the complex mixture of EDCs that occur in daily human life. Further studies using the xenograft mouse model are needed to investigate whether DEHP exposure interferes with the tryptophan-kynurenine-AHR pathway and stimulates tumor growth in vivo (4). The interaction between phthalates and steroid hormones is one of the important areas for future investigation. The inhibitory cross-talk between AHR and steroid hormones has been reported (66). In addition, it is speculated that the effects of DEHP and its metabolites vary by cell and tissue. DEHP showed estrogenic activity in some in vitro and in vivo systems (67, 68), but not in the others (69, 70) or antagonized estradiol-induced estrogen receptor function (71). DEHP is an enhancing-estrogenic chemical rather than a directly estrogenic (72). Li et al. (73) reported that DEHP decreased progesterone levels and induced ovarian granulosa cell apoptosis in mice. However, Crobeddu et al. (74) showed that DEHP and MEHP increased breast cancer cell proliferation through progesterone receptor pathway activation. Progesterone and estrogen, through their receptors, are essential for LM growth (4). Thus, future studies are needed to understand the potential interactions between steroid hormones, phthalates and the AHR pathway in LM growth.

This study explored the association of MEHHP with LM cell growth and did not examine the development of LM. EDCs might induce mutation, such as MED12 or epigenetic changes in myometrial stem cells, leading their transformation into LM stem cells. Numerious xenobiotics, including EDCs, are able to generate reactive oxygen species responsible for oxidative stress (75), which has most recently been shown to drive MED12 mutations in LM (76, 77). Amenya et al. (78) reported that AHR induces epigenetic modification in mouse liver. They showed that dioxin (TCDD) induced DNA demethylation of the AHR target gene, Cyp1a1, through the AHR pathway. Further studies are needed to determine whether MEHHP is associated with tumorigenesis of LM through the AHR pathway.

The present study addresses the effects of phthalate exposure in adult life. In utero or prepubertal phthalate exposure may also predispose women to fibroid development and growth. It is possible that both developmental and adult exposure may be mediated through the AHR or alternative pathways. This is because different exposure windows often use different pathways to exert toxicity. For example, a chemical exposure during development may induce or inhibit one pathway, whereas a chemical exposure during adulthood may inhibit or induce another pathway. Furthermore, the expression of the AHR changes in some tissues during development and adulthood and this could lead to different responses (79, 80)

Our study uniquely links environmental phthalate exposure to LM growth through stimulation of tryptophan metabolism, kynurenine production, and AHR activation. We identified MEHHP exposure as a high-risk factor for LM growth and described a previously unrecognized mechanism by which exposure to environmental phthalate impacts LM pathogenesis. These findings are expected to open new avenues in the uterine LM research field and facilitate the development of novel strategies for the treatment or prevention of the disease.

Materials and Methods

Epidemiological Data Analysis to Evaluate the Associations of Phthalate Metabolite Concentrations with LM Risk. Using data from the MWHS (35), we evaluated bivariable associations between urinary concentrations

of phthalate metabolites with LM diagnosis using a Kruskal–Wallis test to compare geometric mean phthalate metabolite concentrations in women with or without LM. Details about the study, including LM diagnosis, quantification of urinary phthalate metabolite concentrations, and collection of covariate data, were described previously (17). We also assessed associations of urinary concentrations of nine phthalate metabolites (MEHP, MEHHP, MEOHP, MECPP, MCPP, MBzP, MEP, MBP, and MiBP) as a mixture with prior LM diagnosis. We evaluated the overall association of a phthalate metabolite mixture with risk of prior LM diagnosis using WQS regression (WQSR) with repeated holdout approach via Poisson regression and identified which metabolites were the most significant contributors (81, 82). For our analyses, we generated results using 100 repeated holdouts and 100 bootstraps, and data were randomly split into 40% training and 60% validation datasets within each iteration. We converted metabolite concentrations into deciles and constrained WQSR models in the positive direction given our prior results showing that individual phthalate metabolites were associated with a higher risk of prior LM diagnosis. WQSR models accounted for race/ethnicity, income, age at menarche, oral contraceptive use, parity, fertility consultation, and midlife body mass index, and urinary phthalate metabolite concentrations were specific gravity-adjusted. We performed analyses in R Statistical Software (83) using the "gWQS: Generalized Weighted Quantile Sum Regression" (v3.0.4) R package (84).

Materials. The chemicals and pharmacological inhibitors used in this study are listed in *SI Appendix*, Table S4.

Tissue Collection and Primary Cell Preparation. The Institutional Review Board at Northwestern University approved this study. Informed consent was obtained before surgery. Human LM and MM tissues were obtained from premenopausal women undergoing myomectomy or hysterectomy ($n = 48$ [primary cell culture, $n = 29$; RNA extraction from tissues, $n = 19$], mean age [± SD], 43.1 [± 5.1] y; range, 30 to 54 y). These patients had not been subjected to hormonal treatment at least for 3 mo before tissue collection. We did not record the race or ethnicity of these patients. Primary LM and MM cells were prepared as described in previous studies (85). Briefly, fresh tissues were manually cut into small pieces (1 to 2 mm^3), followed by incubation for 5 to 6 h in Hank's buffer containing 1% penicillin/streptomycin (15140122, Sigma-Aldrich), 1.5 mg/mL collagenase type 1 (C0130, Sigma-Aldrich), and 8 mg/mL DNase I (D5025, Sigma-Aldrich) at 37 °C on a shaker. The dissociated cells were cultured in Smooth Muscle Cell Growth Medium-2 (CC-3182, Lonza) with SingleQuozs (CC-4149, Lonza) supplements in humidified air at 37 °C with 5% CO_2. All cells were used within two passages, which produced clinically and functionally relevant molecular results over the past 28 y (86, 87). We used primary cells isolated from five to eight patients for each experiment.

Cell Viability, Cytotoxicity, and Apoptosis Assay (ApoTox-Glo Triplex Assay). The effects of EPI mixture, BAD mixture, MEHHP, and DEHP on viability, cytotoxicity, and apoptosis of LM and MM cells were evaluated by ApoTox-Glo Triplex Assay (G6320, Promega) following the manufacturer's protocol. Briefly, 8,000 to 10,000 cells per well were cultured in 96-well white-walled plates (3610, Corning) overnight. The cells were starved with phenol red-free DMEM/F12 (11039-047, Thermo Fisher Scientific) with 0.2% charcoal-stripped (cs)-FBS for 24 h. Then, cells were treated with vehicle or three different concentrations of phthalates for 48 and 72 h. The detailed doses were described in the corresponding figures and figure legends. Then, 20 μL of viability/cytotoxicity reagent was added to each well and incubated for 30 min at 37 °C, and fluorescence was measured at $400_{Ex}/505_{Em}$ (viability) and $485_{Ex}/520_{Em}$ (cytotoxicity). Next, 100 μL of Caspase-Glo 3/7 regent was added to each well and incubated for 30 min at room temperature, and the luminescence signal was measured for evaluating caspase 3/7 activation, a hallmark of apoptosis. Fluorescence and luminescence were measured by SpectraMax i3.

Total RNA Extraction and Real-Time Quantitative PCR. Total RNA from LM and matched MM tissue or cultured primary LM cells was extracted using the RNeasy Mini Kit according to the manufacturer's instructions (74106, Qiagen). Total RNA was converted to cDNA using the qScript cDNA synthesis kit (95047, Quanta Biosciences). Real-time quantitative PCR (RT-qPCR) was used to determine the mRNA levels of CYP1A1, CYP1B1, AHR, SCL7A5, SCL7A8, and TDO2 on the QuantStudio 5 System (ThermoFisher Scientific) with TaqMan Universal PCR master mix (4304437, Thermo Fisher Scientific). Primers used for PCR are listed in *SI Appendix*, Table S5. The PCR machine was programmed as follows: 50 °C for 2 min and 95 °C for 10 min, followed by 40 cycles of 95 °C for 15 seconds and 60 °C for 1 min. The difference in cycle threshold (ΔCt) was calculated by subtracting the Ct for internal control from the Ct for target genes to determine the relative transcript levels. Hypoxanthine phosphoribosyl transferase 1 (HPRT1) was used as the internal control.

Annexin V-Propidium Iodide Apoptosis Analysis. After reaching 70% confluency, LM cells were starved and treated with 1.6 μM MEHHP for 48 h in phenol red-free DMEM/F12 with 0.2% cs-FBS. Apoptotic cells were measured using the Annexin-V apoptosis detection kit (ab14085, abcam) following the manufacturer's instructions. Briefly, the cells were collected and resuspended in 500 μL of Annexin V binding buffer and incubated with 5 μL of FITC-conjugated Annexin V and 5 μL of propidium iodide for 15 min in the dark. The cells were examined using a BD LSR Fortessa 1 Analyzer and FlowJo software (BD Biosciences).

Cell Cycle Distribution Analysis. LM cells were treated similarly as for Annexin V-propidium iodide (PI) apoptosis analysis. After 48 h of treatment, BrdU was added to the cells and incubated for 24 h. BrdU incorporation was detected using the FITC BrdU Flow Kit (559619, BD Bioscience) following the manufacturer's instructions. Cells were fixed and treated with DNase, and FITC-conjugated anti-BrdU antibody and 7-amino-actinomycin D were added. The cells were examined using a BD LSR Fortessa 1 Analyzer and FlowJo software.

Hydrophilic Metabolite Profiling. The steady-state levels of tryptophan metabolites within the kynurenine pathway (3-hydroxy-anthranilic acid, 3-HK, kynurenic acid, kynurenine, nicotinamide adenine dinucleotide, picolinic acid, QA, tryptophan, XA) were semiquantified by high-performance LC and high-resolution MS and tandem MS (HPLC-MS/MS). LM cells were cultured in 15-cm dishes and treated similarly as described for Annexin V-PI apoptosis analysis. After 72 h of treatment, the cells were harvested with 2 mL 80% methanol on dry ice and lysed with two rounds of incubation at −80 °C for 5 min and vortexing for 60 s. The lysates were stored at −80 °C overnight. Then, the lysates were centrifuged at 20,000 × *g* for 15 min at 4 °C and the supernatants were transferred to new tubes for metabolite analysis. Cell pellets were dissolved in 8M Urea solution, and the protein levels of individual samples were quantified with the BCA Protein Assay kit (23225, Thermo Fisher) for metabolite level normalization. The metabolite levels were analyzed by HPLC-MS/MS at the Northwestern University Metabolomics Core Facility, as described previously (88).

Immunocytochemistry Assay for AHR Nuclear Localization. For the immunocytochemistry assay, 15,000 to 20,000 LM cells were cultured in eight-well chamber slides (354118, BD Falcon) overnight and treated with 10 nM TCDD or 1.6 μM MEHHP for 24 h. Then, the cells were fixed with 4% paraformaldehyde for 15 min followed by permeabilization with 0.1% Triton X-100 in PBS for 15 min on ice. After blocking with 2% BSA in PBS for 30 min, the slides were incubated with antibody (1/100, GTX22770, RPT1, GeneTex) overnight at 4 °C. Then, the slides were incubated for 1 h with secondary antibody Alexa Fluor 488 goat anti-mouse IgG (H+L) (1/500, A-11001, Thermo Fisher Scientific), followed by DAPI (1 μg/mL) nuclear staining. Images were captured using a Leica DM5000 B microscope attached to a Leica DFC450 C digital microscope camera (Leica). The levels of AHR nuclear localization were quantified using NIH ImageJ software (89). The fluorescent signal of the AHR^+ nuclear area was measured and normalized to that of the $DAPI^+$ nuclear area.

Gene Silencing-siRNA Transfection. LM cells were transfected with siRNAs with Lipofectamine RNAiMAX (13778-150, Thermo Fisher Scientific) following the manufacturer's protocol. Briefly, cells were cultured to 70 to 80% confluence. siRNAs were incubated with Lipofectamine RNAiMAX in Opti-MEM (31985, Thermo Fisher Scientific) for 15 min to form complexes, which were then added to the cells cultured in DMEM/F12 or tryptophan-free DMEM/F12 medium (D9807-04, US Biological Life Sciences) with 10% cs-FBS. siRNAs used are listed in *SI Appendix*, Table S5. After a 24-h incubation period, the cells were starved in phenol red-free DMEM/F12 or tryptophan-free DMEM/F12 with 0.2% cs-FBS overnight, followed by treatment with 1.6 μM MEHHP or L-tryptophan (S3987, Selleck Chemicals) for 72 h. Cell viability and apoptosis were evaluated using the ApoTox-Glo Triplex Assay.

Protein Extraction and Immunoblotting Analysis. The cells were treated similarly as in the Annexin V-PI apoptosis analysis. After 24 h of treatment, cells were lysed in radioimmunoprecipitation buffer with protease inhibitor mixture (5871, Cell Signaling Technology) by incubating for 30 min on ice. After centrifugation (14,000 × *g* for 15 min at 4 °C), the protein amount in the supernatant was quantified using BCA Protein Assay kit (23225, Thermo Fisher). Then, the protein was diluted with 4× LDS sample buffer (NP0007, Thermo Fisher), electrophoresed on a NuPage Novex 4–12% Bis-Tris Gel (NP0335BOX, Thermo Fisher), and transferred onto polyvinylidene difluoride membrane (29301-854, VWR International). Primary and secondary antibodies used for immunoblotting are listed in *SI Appendix*, Table S6. Incubation with primary antibodies (AHR, SLC7A5) was performed at 4 °C in 5% nonfat milk (170-6404, Bio-Rad) overnight. Anti–β-actin (ACTB) was used as a loading control. The membranes were then washed and incubated with the appropriate horseradish peroxidase-conjugated secondary antibodies for 1 h at room temperature. Detection was performed by using Luminata Crescendo horseradish peroxidase substrate (WBLUR0500, Millipore) or SuperSignal West Femto Substrate (34096, Thermo Fisher). Immunoblot images were captured by iBright CL1500 imaging system (Thermo Fisher) and each protein was quantified using ImageJ software.

Statistical Analysis for Molecular Studies. All statistical analyses were performed using R software (83). One-way ANOVA followed by Dunnett's test was performed to compare the means of several experimental groups against the control group. Paired Student's *t* test or Wilcoxon signed rank test was performed to compare the means between two experimental groups. The detailed descriptions of statistical analysis are described in each figure legend. The sample size was indicated in the legend and no sample was excluded from the analysis. $P < 0.05$ was considered statistically significant.

Data, Materials, and Software Availability. The data from *in vitro* studies are included in the main text and *SI Appendix*. The Epidemiological data presented in this study are available on request from Jodi A. Flaws. The Epidemiological data are not publicly available because participants did not consent to share data on public websites.

ACKNOWLEDGMENTS. We thank the Northwestern University Flow Cytometry Core Facility and Metabolomics Core Facility, which are cofunded by National Cancer Institute Cancer Center Grant CA060553. This study was supported by NIH Grant P50 HD098580 (to S.E.B. and P.Y.) and the Northwestern Memorial Foundation (P.Y.); US Department of Agriculture National Institute of Food and Agriculture and Michigan AgBioResearch (R.S.S.); and NIH Grant R01 ES026956 (to J.A.F.).

Author affiliations: [a]Division of Reproductive Science in Medicine, Department of Obstetrics and Gynecology, Feinberg School of Medicine, Northwestern University, Chicago, IL 60610; [b]Division of Obstetrics and Gynecology, Department of Clinical Science, Intervention and Technology, Karolinska Institute and Karolinska University Hospital, 171 64 Stockholm, Sweden; [c]Department of Food Science and Human Nutrition, Institute for Integrative Toxicology, Michigan State University, East Lansing, MI 48824; and [d]Department of Comparative Bioscience, University of Illinois at Urbana–Champagne, Urbana, IL 61802

1. S. E. Bulun, Uterine fibroids. *N. Engl. J. Med.* **369**, 1344–1355 (2013).
2. J. J. Kim, T. Kurita, S. E. Bulun, Progesterone action in endometrial cancer, endometriosis, uterine fibroids, and breast cancer. *Endocr. Rev.* **34**, 130–162 (2013).
3. E. R. Cardozo *et al.*, The estimated annual cost of uterine leiomyomata in the United States. *Am. J. Obstet. Gynecol.* **206**, 211.e1–211.e9 (2012).
4. H. Ishikawa *et al.*, Progesterone is essential for maintenance and growth of uterine leiomyoma. *Endocrinology* **151**, 2433–2442 (2010).
5. E. Faerstein, M. Szklo, N. Rosenshein, Risk factors for uterine leiomyoma: A practice-based case-control study. I. African-American heritage, reproductive history, body size, and smoking. *Am. J. Epidemiol.* **153**, 1–10 (2001).
6. E. Diamanti-Kandarakis *et al.*, Endocrine-disrupting chemicals: An Endocrine Society scientific statement. *Endocr. Rev.* **30**, 293–342 (2009).
7. E. Diamanti-Kandarakis, E. Palioura, S. A. Kandarakis, M. Koutsilieris, The impact of endocrine disruptors on endocrine targets. *Horm. Metab. Res.* **42**, 543–552 (2010).
8. CDC, National Report on Human Exposure to Environmental Chemicals (2021). https://www.cdc.gov/exposurereport/index.html (Accessed 6 November 2021).
9. R. T. Benedict *et al.*, *Toxicological Profile for Di (2-Ethylhexyl) Phthalate (DEHP)* (Department of Health and Human Services, Agency for Toxic Substances and Disease Registry, 2022).
10. M. D. Shelby, NTP-CERHR monograph on the potential human reproductive and developmental effects of di (2-ethylhexyl) phthalate (DEHP). *NTP CERHR MON*, v, vii-7, II-iii-xiii passim (2006).
11. J. Högberg *et al.*, Phthalate diesters and their metabolites in human breast milk, blood or serum, and urine as biomarkers of exposure in vulnerable populations. *Environ. Health Perspect.* **116**, 334–339 (2008).
12. H. M. Koch, R. Preuss, J. Angerer, Di(2-ethylhexyl)phthalate (DEHP): Human metabolism and internal exposure–An update and latest results. *Int. J. Androl.* **29**, 155–165, discussion 181–185(2006).
13. C. Chiang, L. R. Lewis, G. Borkowski, J. A. Flaws, Exposure to di(2-ethylhexyl) phthalate and diisononyl phthalate during adulthood disrupts hormones and ovarian folliculogenesis throughout the prime reproductive life of the mouse. *Toxicol. Appl. Pharmacol.* **393**, 114952 (2020).
14. K. A. Richardson *et al.*, Di (2-ethylhexyl) phthalate (DEHP) alters proliferation and uterine gland numbers in the uteri of adult exposed mice. *Reprod. Toxicol.* **77**, 70–79 (2018).
15. A. R. Zota *et al.*, Phthalates exposure and uterine fibroid burden among women undergoing surgical treatment for fibroids: A preliminary study. *Fertil. Steril.* **111**, 112–121 (2019).
16. G. Lee *et al.*, Exposure to organophosphate esters, phthalates, and alternative plasticizers in association with uterine fibroids. *Environ. Res.* **189**, 109874 (2020).
17. D. C. Pacyga *et al.*, Midlife urinary phthalate metabolite concentrations and prior uterine fibroid diagnosis. *Int. J. Environ. Res. Public Health* **19**, 2741 (2022).
18. A. R. Zota *et al.*, Phthalate exposures and microRNA expression in uterine fibroids: The FORGE study. *Epigenet. Insights* **13**, 2516865720904057 (2020).
19. J. H. Kim *et al.*, In vitro effects of phthalate esters in human myometrial and leiomyoma cells and increased urinary level of phthalate metabolite in women with uterine leiomyoma. *Fertil. Steril.* **107**, 1061–1069.e1 (2017).
20. H. J. Kim *et al.*, Effects of phthalate esters on human myometrial and fibroid cells: Cell culture and NOD-SCID mouse data. *Reprod. Sci.* **28**, 479–487 (2021).
21. T. A. Katz, Q. Yang, L. S. Treviño, C. L. Walker, A. Al-Hendy, Endocrine-disrupting chemicals and uterine fibroids. *Fertil. Steril.* **106**, 967–977 (2016).
22. R. S. Pollenz, The mechanism of AH receptor protein down-regulation (degradation) and its impact on AH receptor-mediated gene regulation. *Chem. Biol. Interact.* **141**, 41–61 (2002).
23. U. H. Jin *et al.*, Microbiome-derived tryptophan metabolites and their aryl hydrocarbon receptor-dependent agonist and antagonist activities. *Mol. Pharmacol.* **85**, 777–788 (2014).
24. C. A. Opitz *et al.*, An endogenous tumour-promoting ligand of the human aryl hydrocarbon receptor. *Nature* **478**, 197–203 (2011).
25. M. G. Donovan, O. I. Selmin, D. F. Romagnolo, Aryl hydrocarbon receptor diet and breast cancer risk. *Yale J. Biol. Med.* **91**, 105–127 (2018).
26. S. H. Seok *et al.*, Trace derivatives of kynurenine potently activate the aryl hydrocarbon receptor (AHR). *J. Biol. Chem.* **293**, 1994–2005 (2018).
27. L. F. Bjeldanes, J. Y. Kim, K. R. Grose, J. C. Bartholomew, C. A. Bradfield, Aromatic hydrocarbon responsiveness-receptor agonists generated from indole-3-carbinol in vitro and in vivo: Comparisons with 2,3,7,8-tetrachlorodibenzo-p-dioxin. *Proc. Natl. Acad. Sci. U.S.A.* **88**, 9543–9547 (1991).
28. F. L. Nassan, J. A. Gunn, M. M. Hill, B. A. Coull, R. Hauser, High phthalate exposure increased urinary concentrations of quinolinic acid, implicated in the pathogenesis of neurological disorders: Is this a potential missing link? *Environ. Res.* **172**, 430–436 (2019).
29. T. Fukuwatari, S. Ohsaki, S. Fukuoka, R. Sasaki, K. Shibata, Phthalate esters enhance quinolinate production by inhibiting alpha-amino-beta-carboxymuconate-epsilon-semialdehyde decarboxylase (ACMSD), a key enzyme of the tryptophan pathway. *Toxicol. Sci.* **81**, 302–308 (2004).
30. J. Ernst, J. C. Jann, R. Biemann, H. M. Koch, B. Fischer, Effects of the environmental contaminants DEHP and TCDD on estradiol synthesis and aryl hydrocarbon receptor and peroxisome proliferator-activated receptor signalling in the human granulosa cell line KGN. *Mol. Hum. Reprod.* **20**, 919–928 (2014).
31. A. Shan *et al.*, TCDD-induced antagonism of MEHP-mediated migration and invasion partly involves aryl hydrocarbon receptor in MCF7 breast cancer cells. *J. Hazard. Mater.* **398**, 122869 (2020).
32. D. W. Nebert, Aryl hydrocarbon receptor (AHR): "Pioneer member" of the basic-helix/loop/helix per-Arnt-sim (bHLH/PAS) family of "sensors" of foreign and endogenous signals. *Prog. Lipid Res.* **67**, 38–57 (2017).
33. T. D. Chuang, D. Quintanilla, D. Boos, O. Khorram, Tryptophan catabolism is dysregulated in leiomyomas. *Fertil. Steril.* **116**, 1160–1171 (2021).
34. A. P. Hutchinson *et al.*, Tryptophan 2,3-dioxygenase-2 in uterine leiomyoma: Dysregulation by MED12 mutation status. *Reprod. Sci.* **29**, 743–749 (2022).
35. A. Ziv-Gal *et al.*, The midlife women's health study–A study protocol of a longitudinal prospective study on predictors of menopausal hot flashes. *Womens Midlife Health* **3**, 4 (2017).
36. G. R. Warner *et al.*, Urinary phthalate metabolite concentrations and hot flashes in women from an urban convenience sample of midlife women. *Environ. Res.* **197**, 110891 (2021).
37. Z. B. Zhao *et al.*, Di(2-ethylhexyl) phthalate promotes hepatic fibrosis by regulation of oxidative stress and inflammation responses in rats. *Environ. Toxicol. Pharmacol.* **68**, 109–119 (2019).
38. W. Hu, C. Sorrentino, M. S. Denison, K. Kolaja, M. R. Fielden, Induction of cyp1a1 is a nonspecific biomarker of aryl hydrocarbon receptor activation: Results of large scale screening of pharmaceuticals and toxicants in vivo and in vitro. *Mol. Pharmacol.* **71**, 1475–1486 (2007).
39. A. F. Trombino *et al.*, Expression of the aryl hydrocarbon receptor/transcription factor (AhR) and AhR-regulated CYP1 gene transcripts in a rat model of mammary tumorigenesis. *Breast Cancer Res. Treat.* **63**, 117–131 (2000).
40. R. Devés, C. A. Boyd, Transporters for cationic amino acids in animal cells: Discovery, structure, and function. *Physiol. Rev.* **78**, 487–545 (1998).
41. M. A. Hediger, Y. Kanai, W. S. Lee, R. G. Wells, Identification of a new family of proteins involved in amino acid transport. *Soc. Gen. Physiol. Ser.* **48**, 301–314 (1993).
42. X. Luo *et al.*, Progesterone and mifepristone regulate L-type amino acid transporter 2 and 4F2 heavy chain expression in uterine leiomyoma cells. *J. Clin. Endocrinol. Metab.* **94**, 4533–4539 (2009).
43. Xia Luo *et al.*, LAT1 regulates growth of uterine leiomyoma smooth muscle cells. *Reprod. Sci.* **17**, 791–797 (2010).
44. J. R. Leistico *et al.*, Epigenomic tensor predicts disease subtypes and reveals constrained tumor evolution. *Cell Rep.* **34**, 108927 (2021).
45. M. B. Moyo, J. B. Parker, D. Chakravarti, Altered chromatin landscape and enhancer engagement underlie transcriptional dysregulation in MED12 mutant uterine leiomyomas. *Nat. Commun.* **11**, 1019 (2020).
46. J. W. George *et al.*, Integrated epigenome, exome, and transcriptome analyses reveal molecular subtypes and homeotic transformation in uterine fibroids. *Cell Rep.* **29**, 4069–4085.e6 (2019).

47. S. Bröer, Amino acid transporters as targets for cancer therapy: Why, where, when, and how. *Int. J. Mol. Sci.* **21**, 6156 (2020).
48. L. N. Vandenberg *et al.*, Hormones and endocrine-disrupting chemicals: Low-dose effects and nonmonotonic dose responses. *Endocr. Rev.* **33**, 378–455 (2012).
49. P. W. Albro, R. E. Chapin, J. T. Corbett, J. Schroeder, J. L. Phelps, Mono-2-ethylhexyl phthalate, a metabolite of di-(2-ethylhexyl) phthalate, causally linked to testicular atrophy in rats. *Toxicol. Appl. Pharmacol.* **100**, 193–200 (1989).
50. Y. Ito *et al.*, Species differences in the metabolism of di(2-ethylhexyl) phthalate (DEHP) in several organs of mice, rats, and marmosets. *Arch. Toxicol.* **79**, 147–154 (2005).
51. K. Choi *et al.*, In vitro metabolism of di(2-ethylhexyl) phthalate (DEHP) by various tissues and cytochrome P450s of human and rat. *Toxicol. In Vitro* **26**, 315–322 (2012).
52. R. Mankidy, S. Wiseman, H. Ma, J. P. Giesy, Biological impact of phthalates. *Toxicol. Lett.* **217**, 50–58 (2013).
53. K. Bekki *et al.*, The aryl hydrocarbon receptor (AhR) mediates resistance to apoptosis induced in breast cancer cells. *Pestic. Biochem. Physiol.* **120**, 5–13 (2015).
54. C. F. Vogel *et al.*, Interaction of aryl hydrocarbon receptor and NF-κB subunit RelB in breast cancer is associated with interleukin-8 overexpression. *Arch. Biochem. Biophys.* **512**, 78–86 (2011).
55. C. F. A. Vogel *et al.*, A protective role of aryl hydrocarbon receptor repressor in inflammation and tumor growth. *Cancers (Basel)* **11**, 589 (2019).
56. C. H. Hurst, D. J. Waxman, Activation of PPARalpha and PPARgamma by environmental phthalate monoesters. *Toxicol. Sci.* **74**, 297–308 (2003).
57. D. H. Nam *et al.*, Growth inhibition and apoptosis induced in human leiomyoma cells by treatment with the PPAR gamma ligand ciglitizone. *Mol. Hum. Reprod.* **13**, 829–836 (2007).
58. T.-D. Chuang, D. Quintanilla, D. Boos, O. Khorram, *Further Characterization of Tryptophan Metabolism and Its Dysregulation in Fibroids* (F&S Science, 2022).
59. S. S. Malik, D. N. Patterson, Z. Ncube, E. A. Toth, The crystal structure of human quinolinic acid phosphoribosyltransferase in complex with its inhibitor phthalic acid. *Proteins* **82**, 405–414 (2014).
60. F. L. Nassan, J. A. Gunn, M. M. Hill, P. L. Williams, R. Hauser, Association of urinary concentrations of phthalate metabolites with quinolinic acid among women: A potential link to neurological disorders. *Environ. Int.* **138**, 105643 (2020).
61. L. M. Marshall *et al.*, Variation in the incidence of uterine leiomyoma among premenopausal women by age and race. *Obstet. Gynecol.* **90**, 967–973 (1997).
62. H. M. Eltoukhi, M. N. Modi, M. Weston, A. Y. Armstrong, E. A. Stewart, The health disparities of uterine fibroid tumors for African American women: A public health issue. *Am. J. Obstet. Gynecol.* **210**, 194–199 (2014).
63. M. J. Silva *et al.*, Urinary levels of seven phthalate metabolites in the U.S. population from the National Health and Nutrition Examination Survey (NHANES) 1999-2000. *Environ. Health Perspect.* **112**, 331–338 (2004).
64. J. R. Varshavsky, A. R. Zota, T. J. Woodruff, A novel method for calculating potency-weighted cumulative phthalates exposure with implications for identifying racial/ethnic disparities among U.S. reproductive-aged women in NHANES 2001-2012. *Environ. Sci. Technol.* **50**, 10616–10624 (2016).
65. I. O. Aninye, M. H. Laitner, Uterine fibroids: Assessing unmet needs from bench to bedside. *J. Womens Health (Larchmt.)* **30**, 1060–1067 (2021).
66. P. Pocar, B. Fischer, T. Klonisch, S. Hombach-Klonisch, Molecular interactions of the aryl hydrocarbon receptor and its biological and toxicological relevance for reproduction. *Reproduction* **129**, 379–389 (2005).
67. Y. Nomura *et al.*, Estrogenic activity of phthalate esters by in vitro VTG assay using primary-cultured Xenopus hepatocytes. *Dent. Mater. J.* **25**, 533–537 (2006).
68. M. G. Ter Veld *et al.*, Food-associated estrogenic compounds induce estrogen receptor-mediated luciferase gene expression in transgenic male mice. *Chem. Biol. Interact.* **174**, 126–133 (2008).
69. T. R. Zacharewski *et al.*, Examination of the in vitro and in vivo estrogenic activities of eight commercial phthalate esters. *Toxicol. Sci.* **46**, 282–293 (1998).
70. C. A. Harris, P. Henttu, M. G. Parker, J. P. Sumpter, The estrogenic activity of phthalate esters in vitro. *Environ. Health Perspect.* **105**, 802–811 (1997).
71. M. Ghisari, E. C. Bonefeld-Jorgensen, Effects of plasticizers and their mixtures on estrogen receptor and thyroid hormone functions. *Toxicol. Lett.* **189**, 67–77 (2009).
72. X. Chen *et al.*, Toxicity and estrogenic endocrine disrupting activity of phthalates and their mixtures. *Int. J. Environ. Res. Public Health* **11**, 3156–3168 (2014).
73. N. Li, T. Liu, L. Zhou, J. He, L. Ye, Di-(2-ethylhcxyl) phthalate reduces progesterone levels and induces apoptosis of ovarian granulosa cell in adult female ICR mice. *Environ. Toxicol. Pharmacol.* **34**, 869–875 (2012).
74. B. Crobeddu, E. Ferraris, E. Kolasa, I. Plante, Di(2-ethylhexyl) phthalate (DEHP) increases proliferation of epithelial breast cancer cells through progesterone receptor dysregulation. *Environ. Res.* **173**, 165–173 (2019).
75. P. Sicińska, K. Mokra, K. Wozniak, J. Michałowicz, B. Bukowska, Genotoxic risk assessment and mechanism of DNA damage induced by phthalates and their metabolites in human peripheral blood mononuclear cells. *Sci. Rep.* **11**, 1658 (2021).
76. N. Mäkinen *et al.*, MED12, the mediator complex subunit 12 gene, is mutated at high frequency in uterine leiomyomas. *Science* **334**, 252–255 (2011).
77. Y. Li *et al.*, Myometrial oxidative stress drives MED12 mutations in leiomyoma. *Cell Biosci.* **12**, 111 (2022).
78. H. Z. Amenya, C. Tohyama, S. Ohsako, Dioxin induces Ahr-dependent robust DNA demethylation of the Cyp1a1 promoter via Tdg in the mouse liver. *Sci. Rep.* **6**, 34989 (2016).
79. E. Kimura, C. Tohyama, Embryonic and postnatal expression of aryl hydrocarbon receptor mRNA in mouse brain. *Front. Neuroanat.* **11**, 4 (2017).
80. I. Hernández-Ochoa, B. N. Karman, J. A. Flaws, The role of the aryl hydrocarbon receptor in the female reproductive system. *Biochem. Pharmacol.* **77**, 547–559 (2009).
81. C. Carrico, C. Gennings, D. C. Wheeler, P. Factor-Litvak, Characterization of weighted quantile sum regression for highly correlated data in a risk analysis setting. *J. Agric. Biol. Environ. Stat.* **20**, 100–120 (2015).
82. E. M. Tanner, C. G. Bornehag, C. Gennings, Repeated holdout validation for weighted quantile sum regression. *MethodsX* **6**, 2855–2860 (2019).
83. R Core Team, *R: A Language and Environment for Statistical Computing* (R Foundation for Statistical Computing, Vienna, Austria, 2020).
84. R. Renzetti, P. Curtin, A. C. Just, G. Bello, C. Gennings, *gWQS: Generalized Weighted Quantile Sum Regression* (R Foundation for Statistical Computing, Vienna, Austria, 2021). https://cran.r-project.org/web/packages/gWQS/gWQS.pdf.
85. P. Yin *et al.*, Human uterine leiomyoma stem/progenitor cells expressing CD34 and CD49b initiate tumors in vivo. *J. Clin. Endocrinol. Metab.* **100**, E601–E606 (2015).
86. H. Ishikawa *et al.*, High aromatase expression in uterine leiomyoma tissues of African-American women. *J. Clin. Endocrinol. Metab.* **94**, 1752–1756 (2009).
87. S. E. Bulun, E. R. Simpson, R. A. Word, Expression of the CYP19 gene and its product aromatase cytochrome P450 in human uterine leiomyoma tissues and cells in culture. *J. Clin. Endocrinol. Metab.* **78**, 736–743 (1994).
88. J. Miska *et al.*, Polyamines drive myeloid cell survival by buffering intracellular pH to promote immunosuppression in glioblastoma. *Sci. Adv.* **7**, eabc8929 (2021).
89. C. A. Schneider, W. S. Rasband, K. W. Eliceiri, NIH Image to ImageJ: 25 years of image analysis. *Nat. Methods* **9**, 671–675 (2012).